Astronomy & Astrophysics manuscript no. 22oct˙aa˙ver˙ga January 8, 2004
(DOI: will be inserted by hand later)

Evolution and magnetic topology of the M 1.0 flare of October 22, 2002

A. Berlicki[1,2], B. Schmieder[1,3], N. Vilmer[1], G. Aulanier[1], and G. Del Zanna[4]

[1] Observatoire de Paris, Section de Meudon, LESIA, F-92195 Meudon Principal Cedex, France
[2] Astronomical Institute of the Wrocław University, ul. Kopernika 11, 51-622 Wrocław, Poland
[3] ITA, Oslo, Norway
[4] DAMTP, University of Cambridge, Cambridge, UK

Received date / Accepted date

Abstract. During a coordinated observational campaign between ground based instruments (THEMIS and VTT) and space observatories (SOHO/CDS and MDI, TRACE and RHESSI), an M1.0 flare has been observed mainly during its gradual phase. The objective of this study is to use these multiwavelength observations to study the morphology and evolution of the flare, to analyse the dynamics and energetics of the gradual phase and to understand the role of various heating mechanisms. The RHESSI data allow us to discriminate between thermal and non–thermal processes and the RHESSI spectra indicate that the emission of the flare was mainly of thermal origin with small non–thermal component. During the flare the RHESSI observed emission only within 3 – 25 keV spectral range. The temperature of plasma obtained from the fitting of RHESSI X–ray spectra was between 8.5 and 14 MK. The lower limit of temperature is typical for the plasma contained in "post flare" loops observed in X–rays. The higher temperature was observed at about 16:25 UT during the local maximum of small impulsive feature. The SOHO/CDS observations performed in EUV Fe XIX line also confirm the thermal nature of the radiation. The Fe XIX emission arise at temperatures similar to these obtained from RHESSI spectra (8 – 9 MK). The magnetic topology analysis of the AR by an lfff approach explains the occurence of the flare due to the eruption of a local twisted flux in a sheared magnetic configuration.

Key words. Sun: flares – Sun: X-rays

1. Introduction

The gradual phase of flares can last half an hour to few hours. Detailed observations of flares during their gradual phase have been recorded by SMM and later by Yohkoh (Švestka et al. 1982, Schmieder et al. 1996 and 1997, van Driel et al. 1999?). Soft X-ray instruments in these missions observed the formation of hot loops (10-20 MK). These loops subsequently cool and become visible as post–flare loops in lower temperatures (EUV and Hα lines). The hot loops are formed at higher and higher altitudes as the time is increasing. Such events were interpreted with models based on the Kopp and Pneuman (1976) concept. These models are in two dimensions (Forbes and Malherbe 1986, Forbes and Acton 1996). After the flares, magnetic field lines reconnect at an X point or neutral sheet in the corona. Particles are accelerated as a consequence of the reconnection. Plasma in the loop is heated and chromospheric evaporation occurs at the footpoints of the loops in high density plasma region. These models are well adapted for the interpretation of eruptive events such as two ribbon flares.

During the reconnection process and the gradual phase of flares, SMM with its HXIS telescope could image the high energy particle plasma in four band passes of spectra with a low spatial resolution. The Hard X-ray telescope on–board Yohkoh had a better spatial resolution but no low energy band. A long debate about the long duration emission of particles started in order to understand if the particles accelerated during the impulsive phase were trapped at the reconnection point or if they were continuously accelerated. Ramaty proposed to built an X-ray imager and with possible spectroscopy analysis to distinguish between both processes. The Reuven Ramaty High Energy Solar Spectroscopic Imager (RHESSI: Lin et al. 2002) was launched in 2002 and continuing to operate at the present time, are observing the solar spectrum in the energy range 3 keV – 17 MeV.

We had the opportunity to observe in multiwavelengths a long duration M1.0 flare during a coordinated observational campaign between ground based instruments (THEMIS and VTT) and space observatories

Send offprint requests to: A. Berlicki,
e-mail: arkadiusz.berlicki@obspm.fr

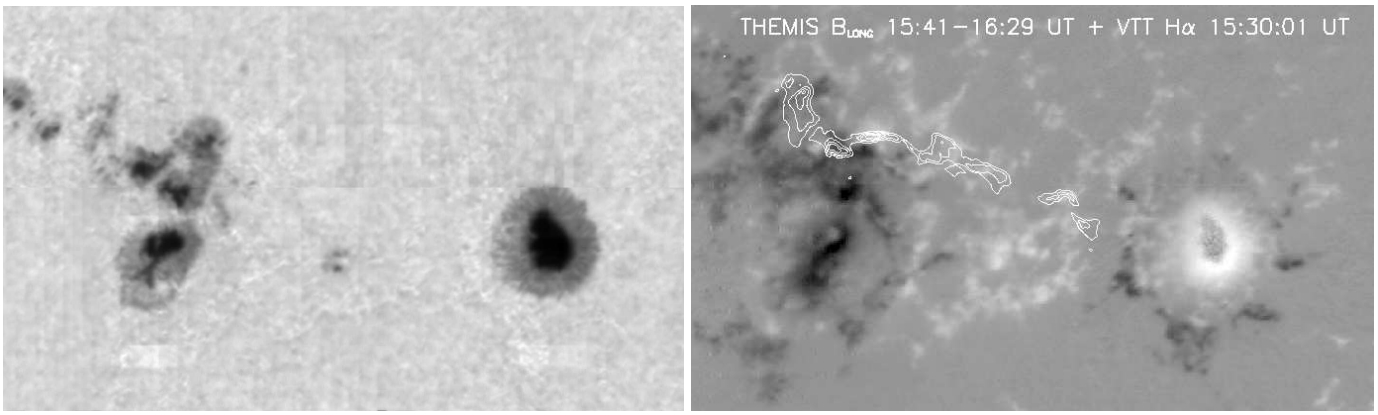

Fig. 1. Image of AR 0162 obtained from THEMIS/MSDP observations taken between 15:41 and 16:29 UT in the Na I D_1 spectral line wing at 200 mÅ from the line center (left panel). In the right panel we present the line-of-sight magnetic field deduced from I and V Stokes profiles at 100 mÅ from the Na I D_1 line centre overlaid with the contours of the Hα flare observed by VTT/MSDP at 15:30:01 UT. The field-of-view (FOV) is 400" × 250".

(SOHO/CDS and MDI, TRACE and RHESSI). The flare followed by several local increases of X–ray emission in its decay phase. This flare occurs in a mainly bipolar active region (as observed by THEMIS). No coronal mass ejection was associated consequently. We observe mainly one long bright ribbon in Hα and with Transition Region and Corona Explorer (TRACE) at 195 Å. To understand the magnetic configuration of the flare we proceed to magnetic extrapolation using the *lfff* (linear force–free field) code developed by Démoulin et al. 1996. Long low sheared horizontal field lines were drawn, they could correspond to the TRACE loops. RHESSI and CDS Fe XIX images show elongated emission over these elongated field lines. This agrees with the models of gradual phase already explained above. The three–dimensional analysis of the extrapolation allows us to have a good idea of the topology of the flare. The analysis of the RHESSI spectra allowed us to find if non-thermal particles can still exist during the gradual phase of the flares.

The paper is organized as follows. In Sect. 2 we describe the observations and their coalignment. In the third section we discuss on the topology of the flare using *lfff* extrapolation. Section 4 provides description and analysis of the RHESSI X-ray spectral observations of the flare. Section 5 summarizes our analysis and provides a description of our results.

2. Observations

The M1.0 flare was observed in NOAA 0162 active region (AR) located about N26 E21 on October 22, 2002. This active region was a target during the coordinated *SOHO* and ground–based observational campaign in October 2002. The active region campaign included EUV spectral observations with the SOHO/CDS Normal Incidence Spectrometer (NIS) (Harrison, 1995). During the passage through solar disk between 17 and 31 October, 2002 the

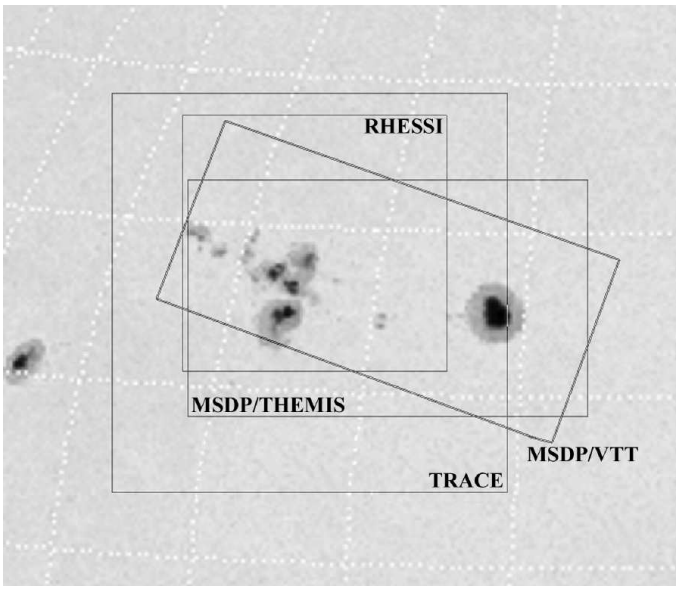

Fig. 2. Approximate orientation of FOVs of different observations used in the analysis of the flare of October 22, 2002. The north is up.

active region consisted of a big leading spot located in positive magnetic field polarity and a cluster of following spots of negative magnetic field polarity (Fig. 1).

According to the GOES 9 flux curve the flare onset was at 15:29 UT and the 1 – 8 Å X-ray flux reached its maximum at 15:36 UT. During the decay phase of this flare there were several local increases of the X-ray flux. The most important one started at about 16:20 UT and reached its maximum at about 16:28 UT.

2.1. Summary of the data

Within X-ray spectral range this flare was observed by GOES 9 and in its decay phase by RHESSI (Lin et al.,

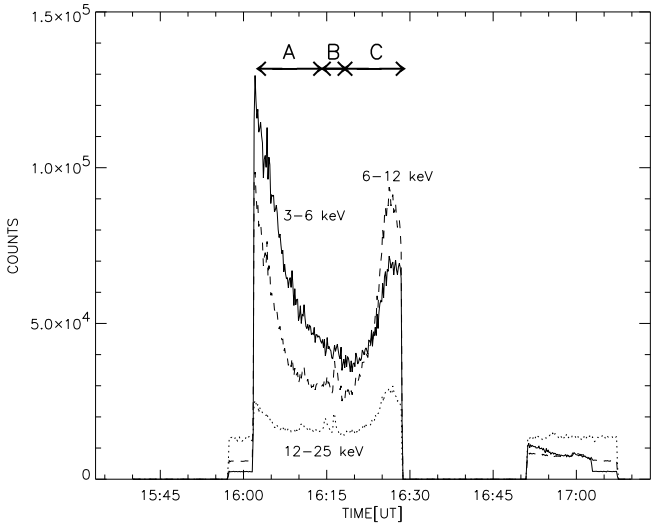

Fig. 3. Time evolution of RHESSI X-ray counts rates observed during the flare of October 22, 2002 in 3–6, 6–12 and 12–25 keV energy bands. The counts rates observed in 12–25 keV energy band were multiplied by a factor of 10 to make the plots more clear. Letters A, B and C denote the phases in the X–ray flux evolution (see Sect. 2.2).

2002). The observations of RHESSI were obtained during the orbit between 16:03 – 16:28 UT. During this time the X-ray emission was detected from 3 keV to about 25 keV.

The spectro-polarimetric observations of the AR 0162 were performed with the THEMIS telescope, operating in the MSDP (Multichannel Subtractive Double Pass spectrograph) observing mode (Mein 2002). On October 22, 2002 we have obtained five scans of the AR 0162. Each scan lasted about 50 minutes. From these scans five set of data were reconstructed. Each set of data consists of the images (400"×250") in the Na D_1 sodium line (intensity, velocity and line-of-sight magnetic field maps at different wavelengths).

In our analysis we also used the VTT/MSDP observations in Hα line (Mein 1991). During the flare between 15:30 and 16:17 UT we completed 9 scans of the MSDP entrance window covering the whole active region with a field-of-view (FOV) of about 380"×170".

During the flare of October 22, 2002, between 15:29 and 15:41 UT, TRACE (Handy et al. 1999) obtained high cadence (40 s) filtergrams in the Fe XII 195 Å line (with a FOV 384"×384" and a 1" resolution), providing information on plasma at 1.5 MK. Before and after this time the TRACE observations were obtained with slightly lower time resolution (50 s) and larger FOV (512"×512"). The solar coordinates of the TRACE images were corrected by using the SOHO/EIT and MDI maps. In the EUV spectral range this flare was also observed by Coronal Diagnostic Spectrometer (CDS) onboard the SOHO satellite.

In Fig. 2 we present the relative pointings and fields of view of the various instruments used in our analysis.

2.2. X-ray observations

Within X–ray spectral range this flare was observed by RHESSI during the orbit between 16:03 – 16:28 UT (Fig. 3). These data allowed us to analyse the images of the flare and the spectra. During this time the flux detected from 3 keV to 25 keV was sufficiently high to perform the reconstruction of the images with spatial resolution of 4" but we needed to use few minutes periods to reconstruct the images with valuable quality. We obtained the images in standard energy bands 3–6 keV, 6–12 keV and 12–25 keV using the CLEAN algorithm with front collimators 3F–9F. During this flare there was no attenuator in the front of the grids.

Analysis of the X–ray flux from RHESSI allowed us to concentrate our analysis on three periods of time (Fig. 3). Between 16:03 and 16:13 UT the X–ray fluxes exhibited a continuous decrease (range A in Fig. 3). At 16:16 UT a weak peak of the fluxes in 6–12 and 12–25 keV bands, lasting about 2 minutes, was observed (range B). After it, from about 16:18 UT we can see continuous increasing of X-ray flux – range C (it reached its maximum at about 16:26 UT, just before the passage of RHESSI through the radiative belts).

Between 16:03 and 16:09 UT during the decaying X-ray flux we could reconstruct the images in 3-6 and 6-12 keV energy bands (Fig. 4-left panel). There was no sufficient emission at higher energies. On these images an elongated loop–like structures are well seen. The positions of these structures were the same on both images made in the two energy bands. On the RHESSI X-ray flux curves (Fig. 3) from about 16:16 UT we can see an increasing flux in all three energy bands. This small event lasted 2 minutes and it was not visible on the RHESSI flux curves for higher energies. During this peak at 16:15–16:19 UT we have reconstructed the images in 3-6 and 6-12 keV energy bands (Fig. 4-middle panel). The X-ray emission was concentrated in two compact sources located slightly to the south of the emission observed at 16:03 UT (Fig. 5 - left panel). In 12-25 keV energy band the flux was too low to make images. After these peaks, from 16:18 UT the flux began to increase. This increase was well visible in 3-6, 6-12 and 12-25 keV energy bands and it reached its maximum at about 16:26 UT, just before the passage of RHESSI through the radiative belts. In the Fig. 4 at this time we can see the elongated loop-like structures which were located to the south of the structures observed at 16:03 and 16:15 UT (Fig. 5 - left panel). The images reconstructed between 16:25 and 16:28 UT in different energy ranges show that there were no significant shifts between the positions of X–ray structures observed at different energies (Fig. 5 - right panel). The increasing emission observed by RHESSI from about 16:18 UT was also detected by GOES 9.

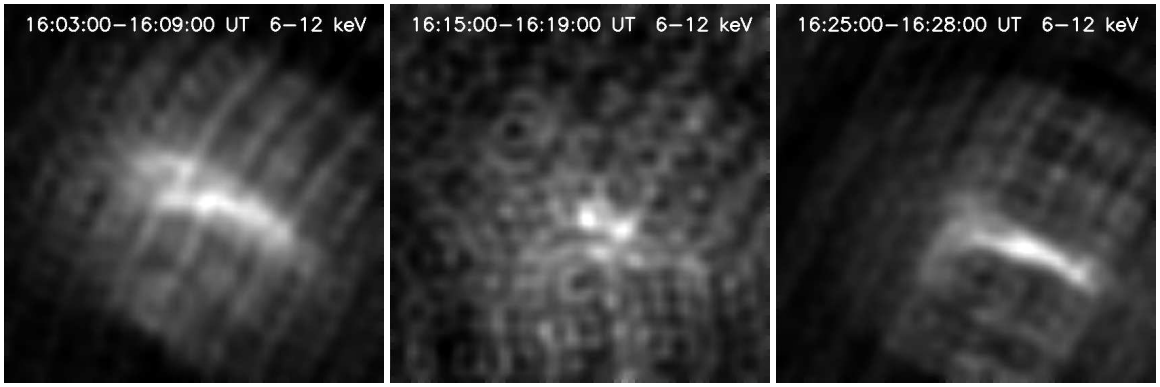

Fig. 4. Sequence of RHESSI images (224" × 224") reconstructed in 6–12 keV energy band during the gradual phase of the flare on October 22, 2002.

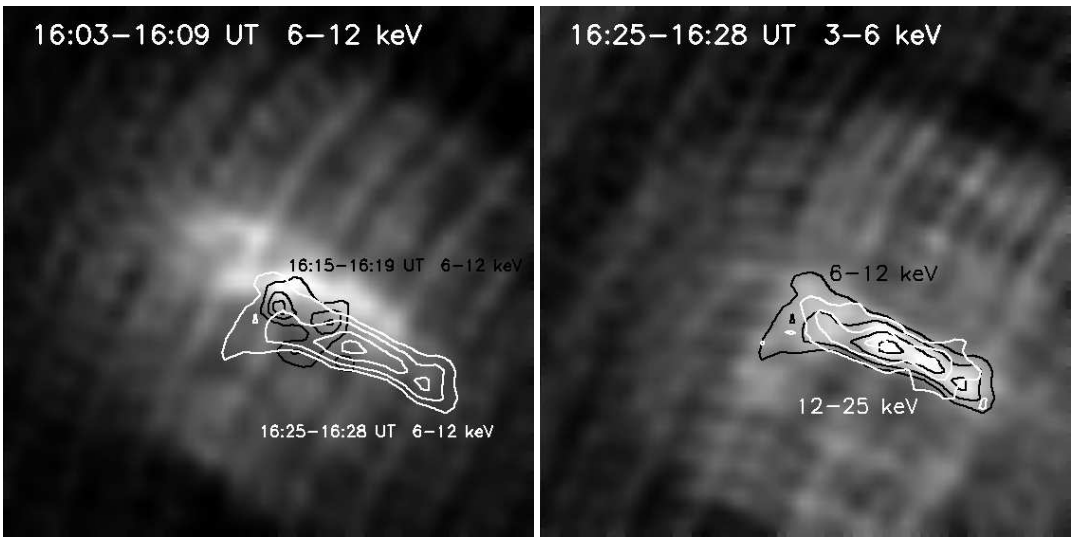

Fig. 5. Left panel: The time evolution of RHESSI X-ray structures observed in 6–12 keV energy band. RHESSI image (224" × 224") taken at 16:03-16:09 UT is overlaid with the contours of X-ray structures observed at 16:15–16:19 and 16:25–16:28 UT. Right panel: The position of RHESSI structures at 16:25–16:28 UT observed in three different (3–6, 6–12 and 12–25 keV) energy band. The image shows the X–ray structures observed in 3–6 keV energy bands overlaid with the contours of the structures observed at this time in 6–12 and 12–25 keV energy bands.

2.3. Magnetic field observation

On October 22, 2002 the spectro-polarimetric observations of the AR 0162 were performed with the THEMIS telescope, operating in the MSDP spectrograph observing mode. THEMIS is a polarization free telescope, designed especially for polarimetric observations. The polarization analyser provides successively the Stokes parameters $I \pm S$ ($S = V$, Q or U) without differential blurring due to seeing effects. Detailed description of the specific instrumental set up of THEMIS in the MSDP observing mode can be found in Mein (2002).

During the flare the observations in Na I D_1 sodium line were performed only for $S = V$ and we obtained the Stokes I and V profiles simultaneously in the 16 MSDP channels. By using these observations the line–of–sight (LOS) magnetic field can be estimated from the observed Stokes profiles. The center-of-gravity method (Semel 1967) was used to determine the magnetic field. In this method the longitudinal component B_l of magnetic field is proportional to the relative shift between the centers of $I + V$ and $I - V$ profiles (for details see the paper of Eibe et al., 2002).

Fig. 1 presents the THEMIS image of AR 0162 obtained in the Na I D_1 spectral line wing at 200 mÅ from the line center (left panel). In the right panel we present the line-of-sight magnetic field deduced from I and V Stokes profiles of the Na I D_1 line. The pixel size of these images is 0.25" but the spatial resolution of the images was limited by seeing (about 1"). The times of the THEMIS images correspond to the beginning of the scans and to obtain one scan it took around 50 minutes. Analysis of all THEMIS images made on October 22, 2002 showed that there were no significant changes of LOS magnetic field configuration during all the day.

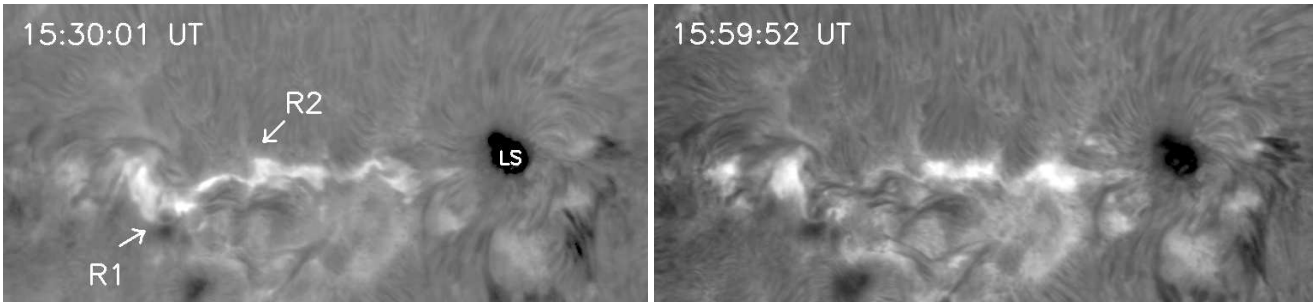

Fig. 6. The flare of October 22, 2002 observed in Hα line by MSDP/VTT spectrograph. The FOV is 340" × 200". R1 and R2 denote the two main ribbons of the flare. LS marks the leading spot of the AR 0162.

2.4. Coronal Diagnostic Spectrometer (CDS)

By rastering the CDS slit (from west to east), monochromatic images and velocity maps of the field of view ($4' \times 4'$) can be constructed. The NIS observes the 305–635 Å spectral range with two gratings, and a spatial resolution of approximately $5''$. The NIS spectral range includes a large number of lines, but due to telemetry limitations, only a limited number of NIS lines are normally extracted and telemetred to the ground. For more details of the CDS see e.g. Harrison et al. (1995) and Del Zanna et al. (2001).

Two types of NIS 'rasters' were used: 1) a slow (1hour 20 mins), diagnostic raster that extracts many diagnostic lines, 2) a fast (20 mins) raster, that only extracts a few lines, selected to cover a wide range of temperatures (He I 522.2 Å, log T = 4.5; O IV 554.5 Å, log T = 5.3; O V 630 Å, log T = 5.4; Mg X 625 Å, log T = 6.0; Si XII 520.8 Å, log T = 6.3; Fe XIX 592.2 Å, log T = 6.9).

The two rasters used the $4'' \times 240''$slit and were repeated a few times over the active region during the day.

CDS observed NOAA 0162 during the periods 08:02–13:07 UT and 15:18–18:33 UT with the two types of rasters. A relatively strong flare was observed during the fast raster taken during 12:43–13:07 UT, approximately in the same location where the M1 flare took place.

The M1 flare that is the subject of this paper was recorded by CDS with a fast raster which scanned the active region between 15:18 and 15:43 UT. CDS also observed the same region with a diagnostic raster (15:43–17:07 UT). The CDS slit was located in the flare area during the peak X-ray emission. It should be noted that spatially-resolved EUV spectroscopic observations of flares are quite rare, although CDS has already observed a number of them, as described in Del Zanna et al. (2002a) and Del Zanna et al. (2002b).

New features which might help in understanding the complex evolution of flares are emerging from the CDS observations. Del Zanna et al. (2002a) presented for the first time spatially-resolved maps of blue-shifts in coronal lines during the decaying phase of a small flare. These blue-shifts were located at the two ends of a small loop system and could be interpreted as related to a slow chromospheric evaporation. This phenomenon is new and should not be confused with the well-known short-duration blue-shifts observed with SMM.

In this paper, only some results concerning these two CDS rasters are presented. A more in-depth discussion of the CDS observations is deferred to a future paper.

A series of standard corrections was applied to the raw NIS data. These include de-biasing, flat-fielding, corrections for the burn-in of the lines, cosmic ray removal. Line intensities were obtained by fitting instrument profiles, following the procedures described in Del Zanna et al. (2001), with a variation that takes into account the fact that after the SOHO loss in 1998 the NIS lines have asymmetric broadened profiles. The CDS pointing has an absolute accuracy of about $5–10''$. Fortunately, CDS simultaneously observes lines emitted over a large range of temperatures, hence CDS data can easily be co-aligned with other data.

2.5. Flare ribbons and coalignments

On the Hα VTT/MSDP images well developed flare ribbons were observed from 15:30 UT. The orientation of two main ribbons R1 and R2 indicates the presence of a large shear in this AR (Fig. 6). The brightest parts of Hα flare ribbons, well visible at 15:30 UT, were much weaker after 7 minutes and almost dissappeared at about 15:59 UT.

On the TRACE sequence taken from 15:30 the first increase of emission in the Fe XIX 195 Å band was observed on the image taken at 15:32:18 UT. The first increase of GOES X-ray flux of M1.0 flare was observed at 15:29 UT. Initially, the emission was concentrated in the compact source well visible at 15:34:56 and 15:40:39 UT (Fig. 7). Later on, from about 15:58:55 UT the TRACE UV emission was concentrated in small, rather low, thin loops spreaded along the axis of the AR and in few brightenings located close to the Hα flare emission (Fig. 8 - lower panels).

At the beginning of the flare the two brightest parts of Hα ribbons were located in the following spots group, each of them in an area of opposite polarity magnetic field (Fig. 1 – right panel).

In this part of the AR the magnetic field gradient was very high and the initial release of the flare energy probably took place here. This idea may be supported by the TRACE 195 Å observations. In the image taken

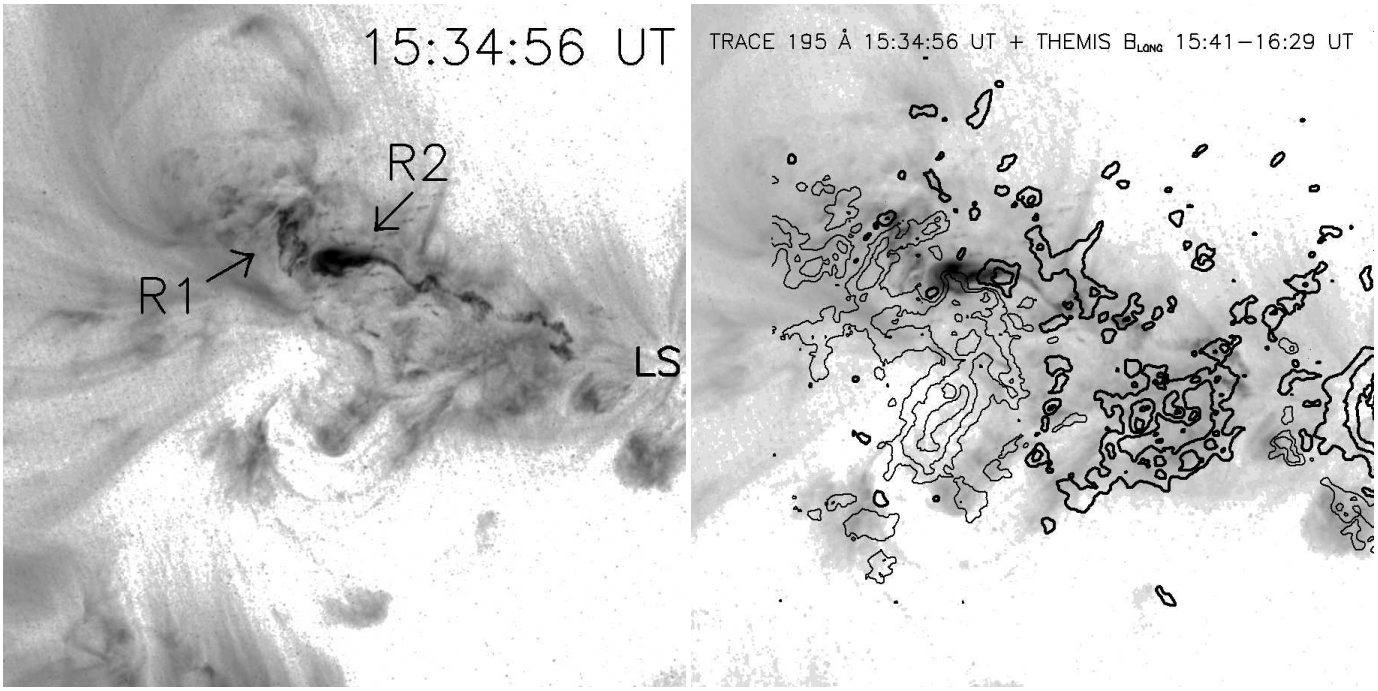

Fig. 7. TRACE 195 Å image of the AR 0162 at 15:34:56 UT. R1 and R2 denote the two main ribbons of the flare and LS marks the leading spot of the AR 0162 (left panel). In the right panel we present the contours of longitudinal magnetic field of the AR 0162 observed with THEMIS in the Na I D_1 spectral line at 15:41–16:39 UT. Thick and thin contours denote respectively the positive and negative polarity magnetic field.

at 15:34:56 UT the brightest UV emission was concentrated just between two Hα flare kernels. In the other VTT/MSDP images taken during the gradual phase between 15:59 and 16:20 UT the Hα flare emission was almost no longer visible at these places but the other parts of the flare ribbons were still bright (Fig. 6).

A similar evolution was seen in the TRACE images. The bright UV emission seen in 15:34:56 UT almost disappeared at 15:58 UT but other UV structures were still in emission (Fig. 8). Fig. 7 (right panel) presents the relative position of the TRACE 195 Å structures observed at 15:35:56 UT overlaid with the contours of LOS magnetic field observed by THEMIS between 15:41 and 16:29 UT.

The coalignment of RHESSI images with the VTT/MSDP filtergrams shows that X-ray emission observed between 16:03 and 16:09 UT is located not on the Hα flare ribbons but, in projection, it is shifted above (Fig. 8 - upper left panel). There is no shift between the emission observed in 3-6 and 6-12 keV energy bands. Later, the X-ray structures observed by RHESSI at 16:25 - 16:28 UT were located (in projection) in the same place as Hα flare emission. In the upper right panel of Fig. 8 we present also the contours of RHESSI X-ray structures observed at three times between 16:03 and 16:25 UT overlaid on THEMIS/MSDP image of LOS magnetic field. In the lower left panel of Fig. 8, the contours of RHESSI image at 16:03-16:09 UT are overlaid on the TRACE image taken at 16:04:38 UT. Note that X-ray emission of the flare is located just above the bright thin loop-like structure seen in UV 195 Å. Later, the X-ray emission observed by RHESSI at 16:25–16:28 UT was located (in projection) just in the same place as TRACE UV emission observed at 16:27:04 UT (Fig. 8 - lower right panel).

During the flare, the Fe XIX line of CDS was very bright (reaching 3000 photon-events in the NIS detector), and clearly shows where strong heating (to at least temperatures of 8 MK) takes place. The peak emission, recorded between 15:35 and 15:43 UT, occurs just above the region of strong mixed polarity, and has a loop-like structure, as more clearly showed by the TRACE 195 Å image (see Fig. 9 - upper left panel). This Fe XIX emission was located also just above strong Hα flare ribbons observed by VTT/MSDP at 15:30:01 UT (Fig. 9 - lower left panel).

Note that the TRACE 195 Å band is dominated at the flare site by Fe XXIV emission, while in general is multithermal, with contributions from plasma at temperatures as low as 700 000 K (see Del Zanna & Mason, 2003)

During the decay phase, the Fe XIX emission becomes more diffuse, a common feature already noted in Del Zanna et al. (2002a, 2002b) and shown in Fig. 9 (right panels) The Fe XIX emission was recorded while the slit was covering the eastern half of the FOV, between 16:20 and 16:51 UT.

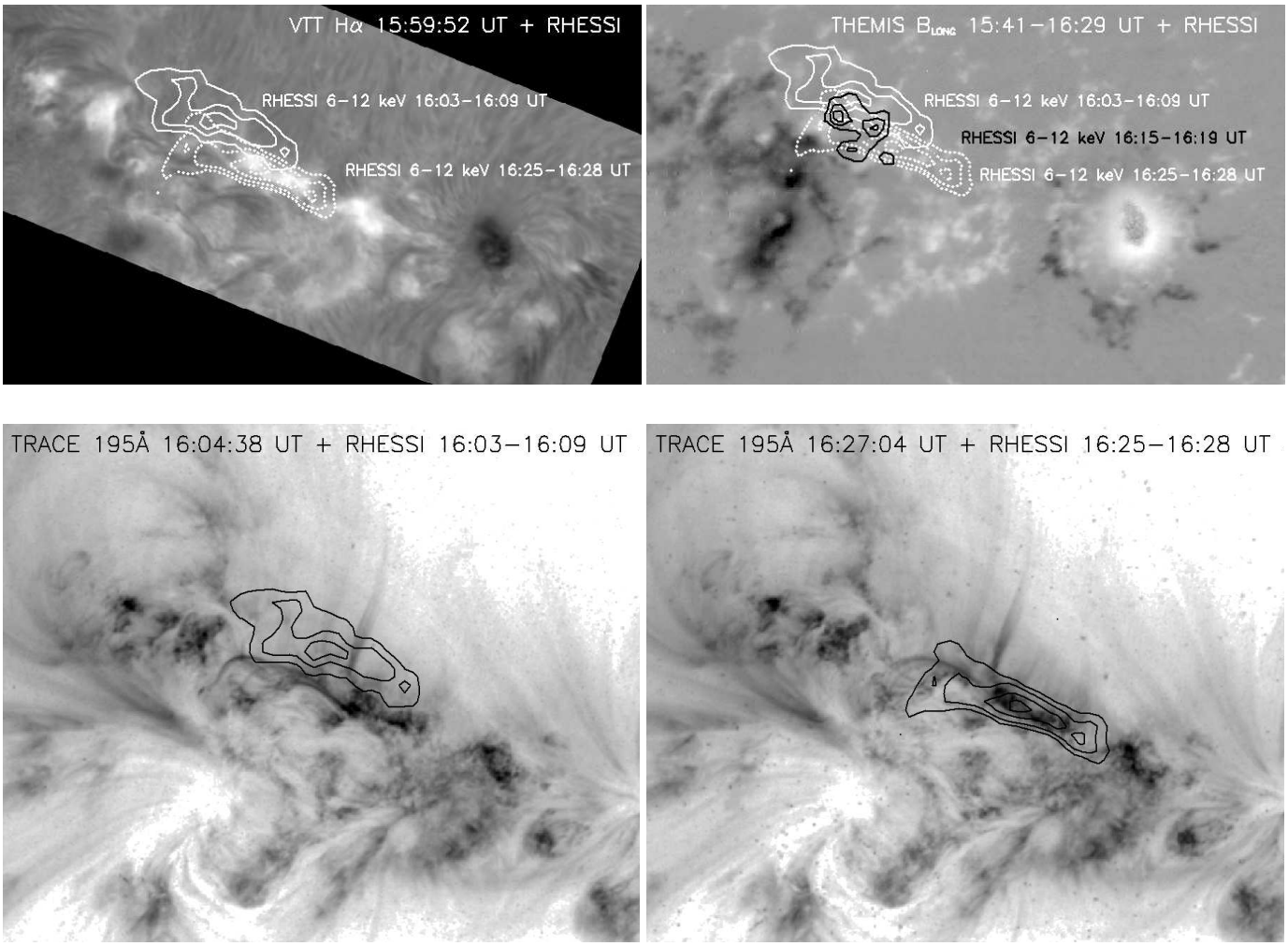

Fig. 8. VTT/MSDP image of the Hα flare in the AR 0162 at 15:59:52 UT (left upper panel) and the longitudinal magnetic field deduced from THEMIS/MSDP observations (15:41–16:29 UT) in the Na I D_1 spectral line at 100 mÅ from the line centre (right panel) overlaid with the contours of the X–ray structures observed by RHESSI at 16:03-16:09, 16:15–16:19 and 16:25–16:28 UT (right upper panel). In the lower panels we present TRACE 195 Å images of the AR 0162 (16:04:38 and 16:27:04 UT) overlaid with the contours of the X–ray structures observed by RHESSI at 16:03–16:09 and 16:25–16:28 UT.

3. Interpretation of the flare in a simple topology

In this section we provide an interpretation for the triggering and the development of the confined flare by the means of a topological analysis of the coronal magnetic field above NOAA 0162 calculated from a linear force-free field model.

3.1. Linear force-free field extrapolation

For the extrapolation, the line-of-sight magnetic fields measured with the THEMIS/MSDP in the Na I D_1 line at 12:32:02 UT were assumed to be equal to the vertical fields at the altitude $z = 0$ (i.e. $\boldsymbol{B}(x, y, z = 0)$) divided by the projection angle, as often done in extrapolations using longitudinal magnetograms only (see e.g. Démoulin et al. 1996, Eibe et al. 2002). The extrapolation was performed in the linear force-free field approximation ($\boldsymbol{\nabla} \times \boldsymbol{B} = \alpha \boldsymbol{B}$ with α = cst) with the FFT method, so with periodic boundary conditions in (x, y) (Alissandrakis, 1981). In order to minimize the boundary effects, a large computational box was chosen, with $\Delta x = \Delta y = 10^3$ Mm, and the magnetic field was computed up to $z = 150$ Mm above the photosphere. The calculation was done with $nx = ny = 1024$ mesh points so as to sufficiently resolve the emerging bipole in the trailing part of the active region. The force-free parameter *alpha* was iteratively tuned so as the obtain a general fit between the orientations of the flare loops observed by TRACE and of the calculated field lines rooted in the vicinity of these loops. This constraint led to fix $\alpha = -5 \times 10^{-3}$ Mm^{-1}, whose sign is compatible with the hemispheric helicity rules found by Pevtsov et al. (1995).

Even though the results of this calculation were used to study the triggering and the development of the flare, we must point out that they are uncertain for two reasons. Firstly, the selected α is equal to 80% of the resonnant value well known for extrapolations performed with a FFT

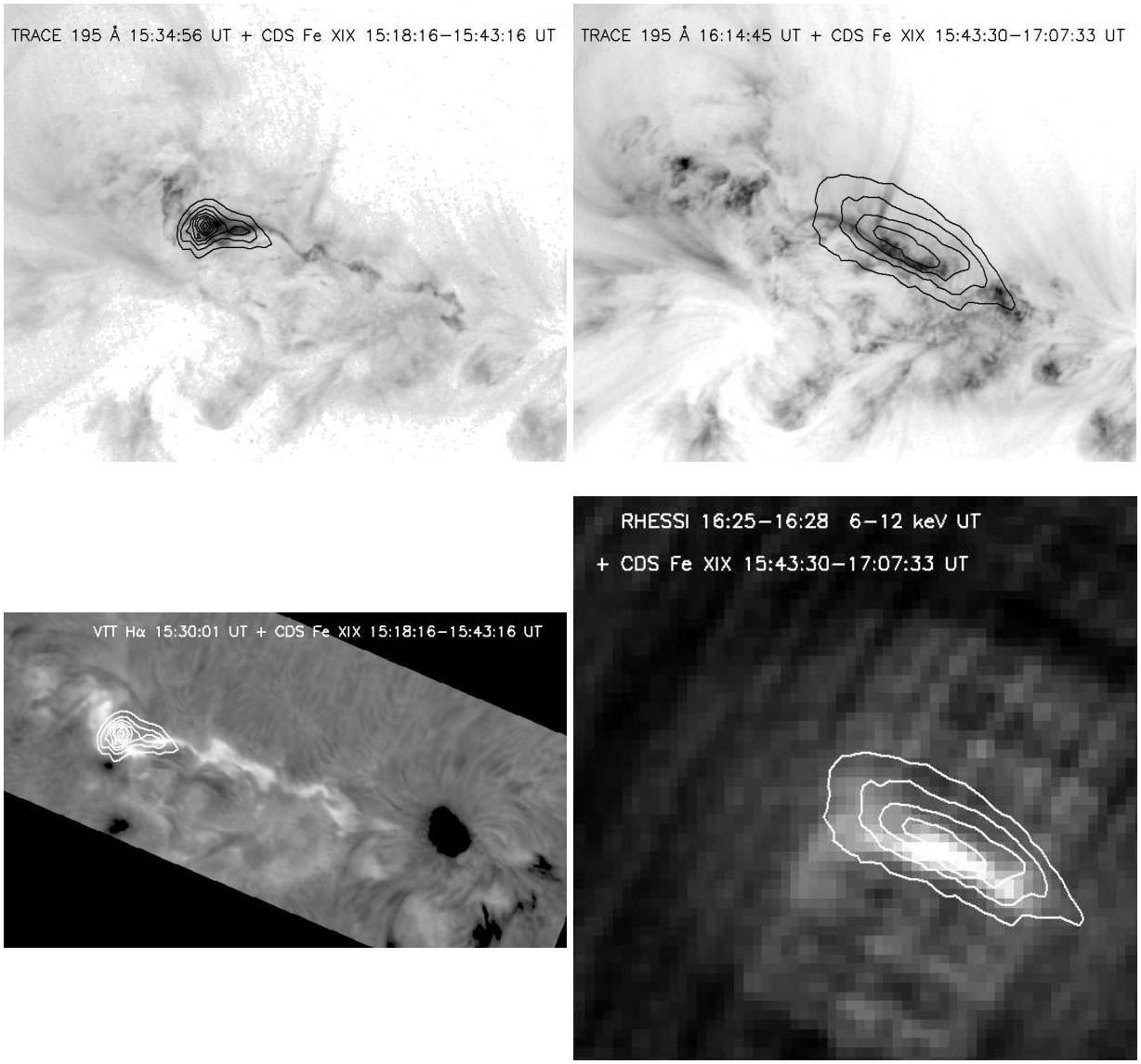

Fig. 9. TRACE 195 Å images of the AR 0162 (15:34:56 and 16:14:45 UT) overlaid with the contours of the UV structures observed by CDS at 15:18:16–15:43:16 and 15:43:30–17:07:33 UT in the Fe XIX line (592.2 Å) (upper panels) and VTT/MSDP image of the Hα flare in the AR 0162 at 15:30:01 UT overlaid with the contours of the UV structures observed by CDS (Fe XIX line, 592.2 Å) at 15:18:16–15:43:16 UT (left lower panel) and RHESSI image (245" × 245") reconstructed for the time 16:25–16:28 UT overlaid with CDS Fe XIX structures observed at 15:43:30–17:07:33 UT (right lower panel).

in a large computational box. This leads to a very probable artificial over-shearing of the large scale loops. Secondly, it was impossible to find a single value of α with, even in a 20% interval, which allowed to fit all the observed TRACE loops with calculated magnetic field lines. Therefore, it appears that the α =cst hypothesis of the *lfff* extrapolation may be strongly disputed in this region. Nevertheless, as the global magnetic topology is a well preserved property of magnetic fields since it is an intergral quantity, we still used the *lfff* model to pursue our analysis, although it is clear that it is disputable on small scales (where electric currents are concentrated) and on large scales (where the field is too much sheared).

3.2. Origins of the asymmetrical ribbons

Figure Fig. 10 shows the results of the *lfff* extrapolation. The large scale shear is evident on the scale of the full active region, as seen on the *top left* pannel. The other pannels show the connectivies of the magnetic field lines in the vicinity of the emerging bipole and around the flare ribbons as observed in Hα.

In this region, even though a few nulls points are present around the negative moving magnetic features on the edges of the leading spot, the global topology is *not* complex : no thin quasi-separatrix layers were found to be associated with the flare loops, contrary to many previous studies of confined flares (see e.g. Mandrini et al. 1996, Schmieder et al. 1997, Aulanier et al. 2000). Also,

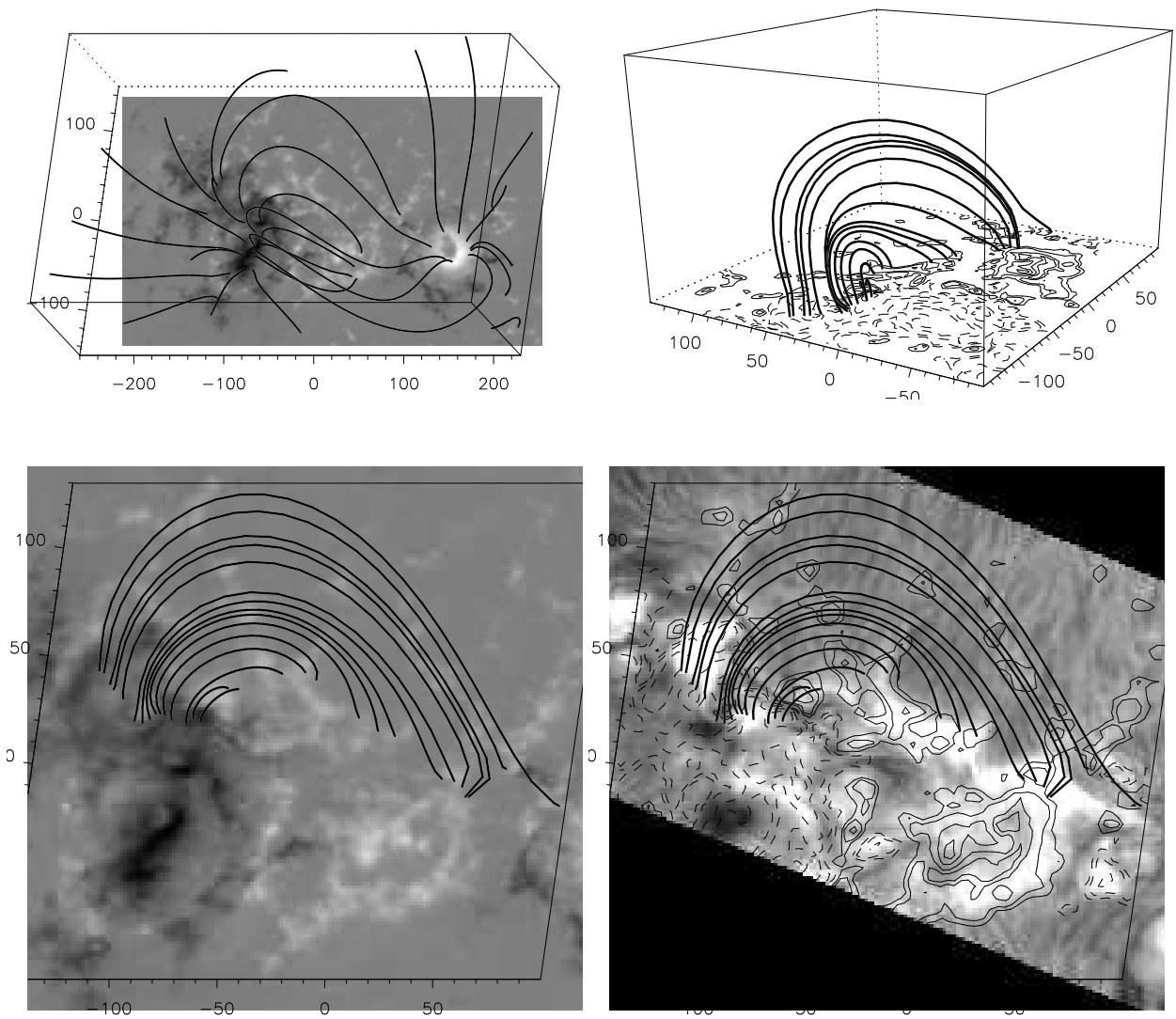

Fig. 10. (*top left:*) superposition of the THEMIS/MSDP Na D1 magnetogram of 12:32:02 UT with a sample of magnetic field lines resulting from the *lfff* extrapolation. (*bottom right:*) partial view of the flare as observed in Hα with the VTT/MSDP at 15:59:52 UT. the field lines are the ones which are rooted in the flare ribbons R1 and R2 as well as in the emreging bipole. (*bottom left:*) same as *bottom right*, except that the underlying image is the THEMIS magnetogram. (*top right:* projection view of the field lines shown in the *bottom* pannels. Continuous (resp. dashed) contours stand for positive (resp. negative) vertical fields. North is toward the left.

the connectivities look very continuous around the region of the emerging bipole. So at first sight it appears that the flare studied in this paper cannot be interpreted with the standar reconnexion model. However emerging bipoles are known to often emerge twisted (Leka et al. 1995, Lopez-Fuentez et al. 2000), which is supported by the Huairou vector magnetograms for this region (Y.H. Yan, privated communication). Therefore we conjecture that the flare was still probably due to magnetic reconnexion, but here between small scale twisted emerging fields (not calculated in the extrapolation) and the large scale sheared magnetic fields of the global bipole of NOAA 0162. Since the flare was confined, it may then be interpreted by the global disruption model calculated by Amari et al. (1999) in a very symetrical configuration, where a very locally twisted flux tube undergoes an ideal kink instability and reconnects with overlaying potential fields.

If we assume the global disruption scenario, the *lfff* model naturally provides an explanation for the appearance of the compact ribbon R1 and its elongated counterpart R2, as well as its fast propagation away from the emerging bipole and toward the leading sunspot. Figure 10 indeed shows that the field lines located higher and higher above the emerging bipole are rooted in R1 and R2, and have footpoint separations that are small on the R1 side and quite large on the R2 side. The reconnexion of the growing emerging fields with higher and higher overlaying fields sequentially provides a natural explanation for the

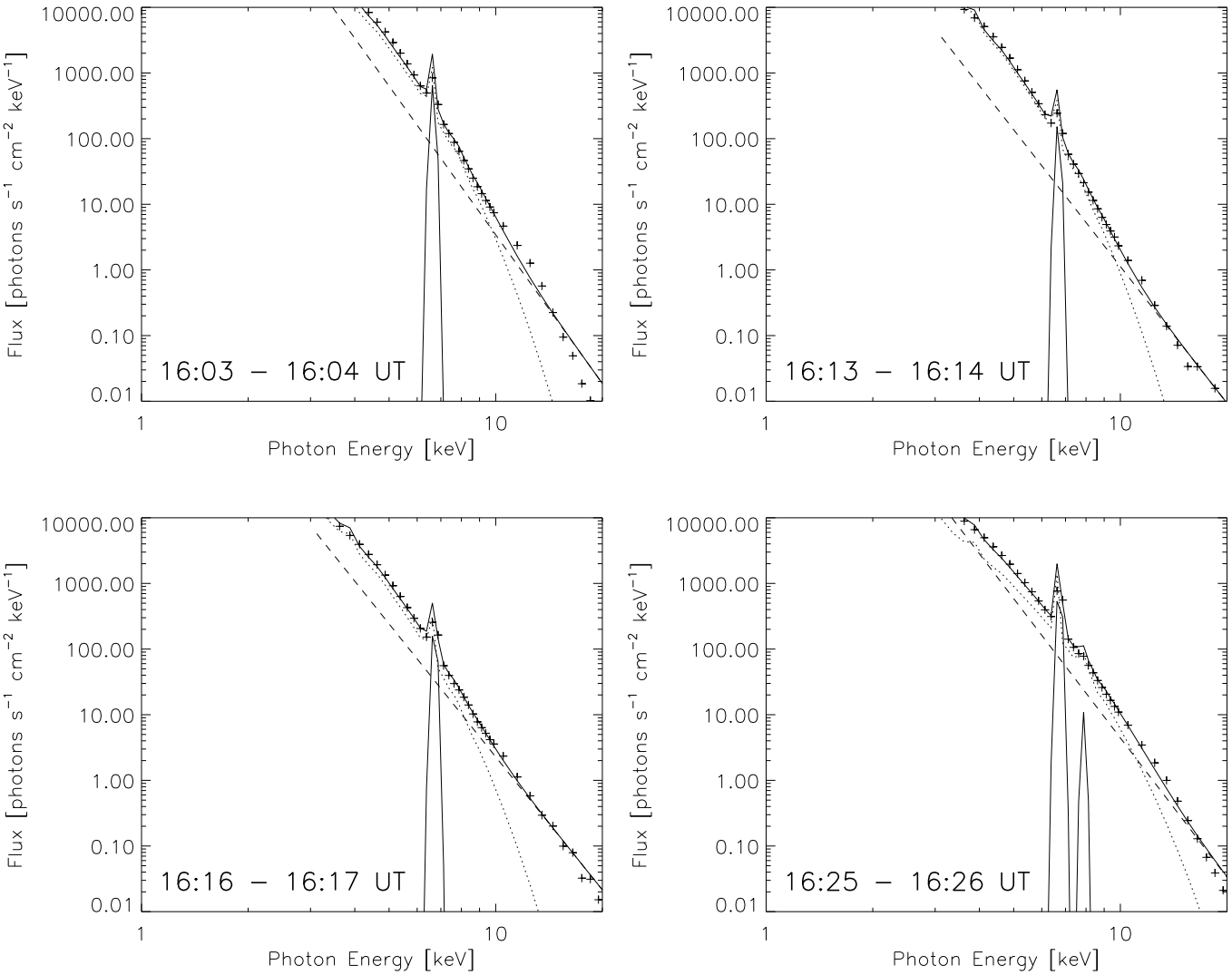

Fig. 11. RHESSI spectra reconstructed during the gradual phase of the solar flare in four times: 16:03–16:04, 16:13–16:14, 16:16–16:17 and 16:25–16:26 UT. Dotted lines denote the calculated thermal component, dashed lines represent non–thermal component, thin continuous lines are the Fe XXV line (6.969 keV) calculated in our model. In our modelling of the specrum at 16:25–16:26 UT we also used other Fe XXV line (7.876 keV). Thick continuous lines are the sum of all components – predicted photon spectum. With crosses we marked observed flare spectrum.

sequential brightening of their footpoints along the flare ribbons, included along the very elongated R2 ribbon. In this frame, the fast propagation of the brightenings as observed by TRACE are not due to MHD waves, but are rather due to the electrons beams accelerated from the reconnexion regions above the emerging bipole in the long overlaying loops of NOAA 0162, which progressively reach larger and larger chromospheric areas toward the West.

It is also noteworthy that the shape of the field lines anchored in the Hα ribbons follows the elongated shape of the RHESSI images recorded in the $6 - 12$ keV range of energy between 16:03-16:09 UT. Thus the extrapolation supports the idea that RHESSI permits to see thermal emission of coronal loops heated by the confined flare, though it is not contradictory with a possible non-thermal component since its is known that reconnexion can accelerate particules along reconnected field lines. The RHESSI emission at 16:25-16:28 UT being similar in shape to the one recorded at 16:03-16:09 UT, though slightly shifted southward, suggests that this secondary event may be associated to the resistive relaxation of the system which may have been forced too rapidly by the flare of 15:59 UT, as in the reconnexion calculations of Karpen et al. (1998). Unfortunately, the present data and model cannot provide more clue to this issue.

4. RHESSI X–ray spectra of the flare

Using the RHESSI data and SPEX package we also performed the analysis of spectra obtained from the data taken between 16:03 and 16:27 UT. To substract the background emission we used the data taken before the flare

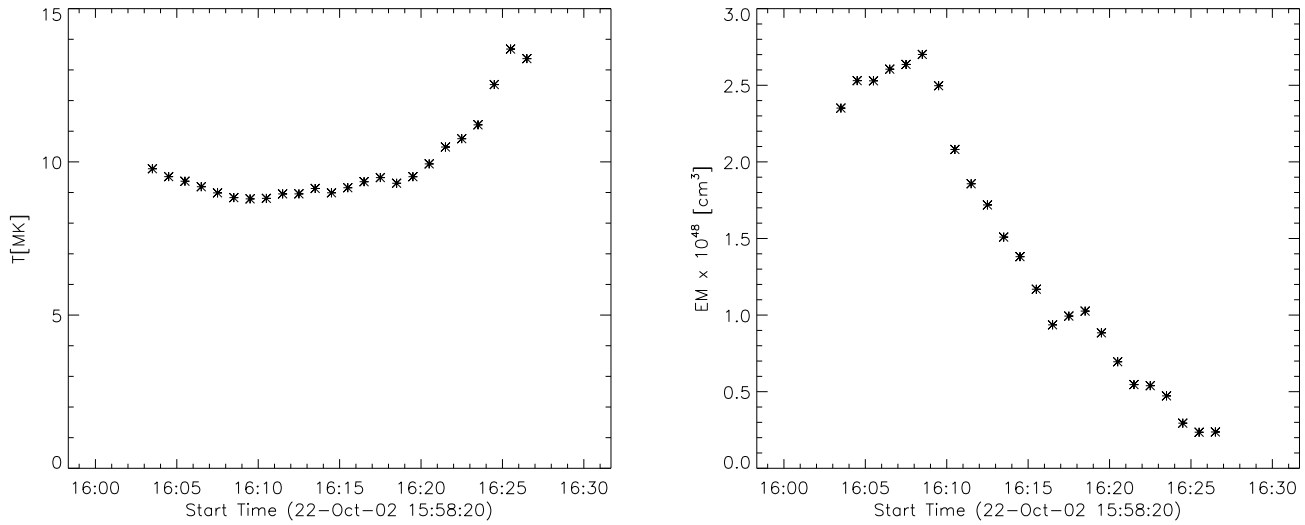

Fig. 12. The time evolution of the temperature T and emission measure EM of the flare on October 22, 2002 These parameters were obtained from the fitting the observed RHESSI spectra.

during the previous RHESSI orbit at 15:12–15:24 UT. Then, we made the spectra for all 1 minute time bins between 16:03 and 16:27 UT. For the spectra we used modified binning code No. 14. To increase the spectral resolution of spectra, instead of 1 keV energy bins, between 3 and 10 keV we have used 0.25 keV energy bins. To make a spectra we used the collimators 1F – 9F, except 2F and 7F. We omitted the data from these detectors because they have a poorer energy resolution than intended (Smith et al. 2002). We performed the full calculations of all diagonal and off-diagonal matrix elements.

Using the procedures of SPEX package we have reconstructed the spectra for different periods in time. All the spectra made between 16:03 and 16:27 UT exhibited similar distribution of the energy from 3 to 10 keV. In this range we could fit them by using thermal model F-VTH taken from the SPEX package. On the spectra plotted both in counts and photon scale the spectral line of Fe XXV (6.696 keV) was well seen. Above about 10 keV the observed spectra did not follow the thermal model and we could fit this part of the spectra using non-thermal model. Finally, we performed the fitting of the whole spectra using F-VTHC-BPOW-NLINE model. In our fitting procedure we used the data contained within the energy range 3.0 – 20 keV. This model is a mixture of thermal and non-thermal components together with the line of given intensity, wavelength and width. In our fitting procedure we have used the line which describe the Fe XXV emission (6.696 keV). For the spectra reconstructed during the increase of X-ray flux at about 16:26 UT we introduce another line–feature at the energy of 7.876 keV. The spectra made between 16:03 and 16:27 UT differs mainly in the contribution of non-thermal radiation to the spectrum above the 10 keV energy. In the period 16:03 – 16:13 UT the spectra were more thermal in comparison with the spectra made during the peak of X–ray flux at 16:16 – 16:18 UT or during the increasing of the radiation observed from about 16:18 UT. The non-thermal component gave the largest input during the maximum of X-ray flux at about 16:26 UT. Fig. 11 presents the RHESSI X-ray spectra reconstructed in four characterictic times. All spectra are similar and characteristic for the gradual phase of the flare where the non–thermal component has a very low input.

In the Fig. 12 we can see the time evolution of the temperature T and emission measure EM obtained by the fitting of the observed spectra with the model F-VTHC-BPOW-NLINE. First, the observed temperature decreases from about 9.7 MK to 8.8 MK and after, at 16:10 UT starts to increase to the value of 13.6 MK. It means that from about 16:10 UT some heating processes took place. Just at 16:10 UT the emission measure started to decrease from about $2.53 \times 10^{48} cm^{-3}$ to $2.35 \times 10^{48} cm^{-3}$.

5. Conclusions

The multiwavelength observations of an M1.0 flare on October 22, 2002 obtained during its gradual phase allowed us to perform a complex analysis of the morphology and to understand the mechanisms which are responsible for observed evolution of this event. The magnetic field (photospheric and extrapolated) and the aligned Hα ribbons shows that this active region is highly sheared, thus stores energy. The break-out of the flare occurs in the region of high gradient of B which could correspond to the emergence of a locally very twisted magnetic flux. The *lfff* extrapolation of the magnetic field provides an explanation for the appearance two Hα flare ribbons. Ribbon R1 was compact and the its position was almost constant during the flare. Ribon R2 was elongated and exhibited fast propagation from the emerging bipole towards the leading sunspot.

Hα and TRACE observations show the development of two bright ribbons going away from each other versus time. This agrees with the model already accepted for gradual phase of flare (Forbes and Malherbe, 1986, Forbes and Acton, 1996). During the decay phase, X-ray was observed above the post-flare loops at the reconnection site of magnetic field lines. This emission originated from trapped particles or continuous reconnection processes. There was no X-ray emission at the footpoints of the loops which indicate that there was no non–thermal heating of Hα flare ribbons. The thermal conduction heating can be responsible for the TRACE ribbons but is not sufficient to explain the Hα flare emission (Berlicki and Heinzel 2004). We need to investigate other processes for instance the effect of high coronal pressure.

The RHESSI observations performed during the gradual phase of this flare suggests that the X–ray emission observed above the active region had a thermal nature. The RHESSI spectra showed that the contribution of non–thermal emission to the total X–ray flux is not strong. From the fitting of RHESSI spectra we found the temperature of flare plasma which is not high (around 9–14 MK) and typical for the structures observed during the gradual phase of solar flares. The CDS observations in Fe XIX line (592.2 Å) performed at 15:43:30–17:07:33 UT confirm the thermal nature of the radiation. The CDS Fe XIX emission arise at the temperature around 8–9 MK which is in agreement with the temperatures obtained from the RHESSI spectra. Besides, the EUV emission was located in the projection in the same place as RHESSI X-ray emission. The intensity of X–ray lines used in fitting the RHESSI spectra support the thermal nature of X-ray emission. The Fe XXV line (6.696 keV) indicate the presence of high temperature plasma (about 9–10 MK) (Phillips, 2003). At 16:26 UT, during the local increase of X–ray flux we observe that another line–feature appeared at 7.876 keV. This line emission resulting from the increasing of the temperature which rise to about 14 MK.

Acknowledgements. The magnetic field extrapolations used in this paper have been obtained from the code base FRench Online MAGnetic Extrapolations (FROMAGE). FROMAGE is a joint project between LESIA (Observatoire de Paris), CPhT (Ecole Polytechnique) and the Centre National d'Etudes Spatiales (CNES). The work of AB was supported by the European Commission through the RTN programme (European Solar Magnetism Network, contract HPRN-CT-2002-00313). VTT/MSDP observations have been provided and reduced by P., N. Mein and J. Staiger. These observations were performed during a MEDOC campaign (JOP 157). GDZ acknowledges support from PPARC (UK). The TRACE analysis at SAO is supported by a contract from Lockheed Martin.

References

Alissandrakis 1981
Amari et al. 1999
Aulanier, G. et al. 2000
Berlicki, A., & Heinzel, P. 2004, A&A- accepted
Del Zanna, G., Bromage B. J. I., E. Landi, E. & Landini, M. 2001, A&A, 379, 708
Del Zanna, G., Mason, H. E., Gibson, S. E., Pike, C. D., & Mandrini, C. H. 2002a, Adv. Space Res., Vol. 30, No. 3, 551
Del Zanna, G., Mason, H. E., & Foley, C. 2002b, Proc. 10th European Sol. Phys. Meeting, ESA-SP 506, 585
Del Zanna, G., Mason, H. E. 2003, A&A, 406, 1089
Démoulin, P. et al. , 1996
Démoulin, P. et al. , 1997
Eibe, M. T., Aulanier, G., Faurobert, M., Mein, P. & Malherbe, J. M. 2002, A&A, 381, 290
Forbes, T. G. & Acton, L. W. 1996, ApJ, 459, 330
Forbes, T. G. & Malherbe, J. M. 1986, ApJ, 302, L67
Handy et al. 1999
Harrison, R. A., et al. 1995, Sol. Phys., 162, 233.
Karpen et al. 1998
Kopp, R. A. & Pneuman, G. W. 1976, Sol. Phys., 93, 351
Leka et al. 1995
Lopez-Fuentez et al. 2000
Mandrini et al. 1996
Mein, P. 1991, A&A, 248, 669
Mein, P. 2002, A&A, 381, 271
Lin, R. P. 2002, Sol. Phys., 210, 3
Pevtsov et al. 1995
Phillips, K. J. H. 2003, ApJ, 000, 000
Schmieder, B, Heinzel, P., Van Driel-Gesztelyi, L. & Lemen, J. R. 1996, Sol. Phys., 165, 303
Schmieder, B. et al. 1997
Semel, M. D. 1967, Ann. Astroph., 381, 271
Smith et al. 2002
Švestka et al. 1982
Van Driel, L., et al. 1999